

Towards Markov-State Holography

Xizhu Zhao,¹ Dmitrii E. Makarov,^{2,3} and Aljaž Godec^{1,*}

¹*Mathematical bioPhysics Group, Max Planck Institute for Multidisciplinary Sciences, 37077 Göttingen, Germany*

²*Department of Chemistry, University of Texas at Austin, Austin, Texas 78712, USA*

³*Oden Institute for Computational Engineering and Sciences,
University of Texas at Austin, Austin, Texas 78712, USA*

Experiments, in particular on biological systems, typically probe lower-dimensional observables which are projections of high-dimensional dynamics. In order to infer consistent models capturing the relevant dynamics of the system, it is important to detect and account for the memory in the dynamics. We develop a method to infer the presence of hidden states and transition pathways based on observable transition probabilities conditioned on history sequences for projected (i.e. observed) dynamics of Markov processes. Histograms conditioned on histories reveal information on the transition probabilities of hidden paths *locally* between any specific pair of observed states. The convergence rate of these histograms towards a stationary distribution provides a *local quantification of the duration of memory*, which reflects how distinct microscopic paths projecting onto the same observed transition decorrelate in path space. This provides insight about the hidden topology of microscopic paths in a holography-like fashion. The method can be used to test for the local Markov property of observables. The information extracted is also helpful in inferring relevant hidden transitions which are not captured by a Markov-state model.

Many processes in complex, especially living, systems are described as Markovian diffusion on an energy landscape [1–3], or—at the longest timescales—as continuous-time Markov jump processes [4–6]. Experiments, however, typically probe low-dimensional observables, which are projections of high-dimensional dynamics that are “blind” to hidden degrees of freedom [7–18]. The observed dynamics therefore displays memory (i.e. is non-Markovian) whenever the hidden degrees of freedom do not relax much faster than the observed ones [19–35]. In such a non-Markovian process, the state changes depend not only on the current state but also on the past.

The typical way to account for memory in continuous-space systems is via generalized Langevin equations, which require the (highly non-trivial) sampling and parameterization of a potential of mean force and a memory kernel [16, 28–32, 36, 37]. A widely adopted strategy to account for hidden states in discrete-state systems are Hidden-Markov Models (HMMs) [38]. However, HMMs inherently rely on explicit assumptions about the underlying model, which, especially because of limited sampling and over-fitting [39] as well as Bayesian prior-dependence [40, 41] give rise to hard challenges in model selection. “Model-free” inference methods—in the present context, methods that make *no* assumptions about the underlying topology and number of states in the network and do *not* require a Markov model to even be parameterized—are therefore desired.

Several approaches have been developed to infer and quantify memory from time-series in a model-free manner [15, 33, 42–47]. One common approach for testing for Markovianity is examining the distribution of the waiting times in each observed state [12, 48–50]. However, exponentially distributed waiting-times are only a necessary

but *not* a sufficient condition for a process on a discrete state space to be Markovian. While a non-exponential waiting time distribution certainly indicates memory, the converse is *not* true; it is easy to construct non-Markov models with exponential waiting time distributions [51]. More sensitive methods exploit the statistical properties of transition-path times to infer the existence of hidden transition pathways [42–44], test for violations of the Chapman-Kolmogorov (i.e. semigroup) property [15, 45, 47], or use Shannon’s information-theoretical approach to detect memory in observed time series [46]. However, such approaches test for non-Markovianity of the entire observed time series, and none of these methods can detect and quantify memory *locally*.

In related studies, great efforts have been made in the context of thermodynamic inference from coarse and partial observations [50, 52–63]. In particular, the existence of the so-called “Markovian events”—states, or transitions between states where the microscopic is fully observable—have proven to be a crucial assumption in many methods of thermodynamic inference [50, 59, 60]. But since such Markovian events are local properties of the observed dynamics, it again remains elusive to reliably (and conclusively) detect them. More even than the practical need to analyze experimental data, we face the fundamental question: *Can one infer the presence of hidden parallel transitions between specific observed states locally without specifying an underlying model?* This would also provide an important step towards detecting Markovian events.

Here, we develop a method to quantify the extent of memory *locally* between any pair of observed states based on the defining Markov property. This method allows one to infer the presence of hidden states and transition channels from observed trajectories in a *holographic* and model-free manner. The holography-like inference exploits how the transition probability between pairs of

* agodec@mpinat.mpg.de

observed states depends on the history.

Setup.—We consider the full dynamics to be an m -state continuous-time Markov-jump process with generator $\mathbf{L} = \{L_{\alpha\beta}\}$, whose off-diagonal elements $L_{\alpha\beta}$ are transition rates from state β to α , and diagonal elements are $L_{\alpha\alpha} = -\sum_{\beta \neq \alpha} L_{\beta\alpha}$. We only consider the the sequence of visited states and discard the waiting times between transitions. The resulting microscopic sequence is a discrete-time Markov chain with the transition matrix $\Phi = \{\Phi_{\alpha\beta}\}$ given by the splitting probabilities $\Phi_{\alpha\beta} = -L_{\alpha\beta}/L_{\beta\beta}$ ($\alpha \neq \beta$), and $\Phi_{\alpha\alpha} = 0$. Waiting times may easily be analyzed separately; if these are non-exponentially distributed this implies memory.

We assume that some microscopic states are projected onto the same observable state, i.e. are not distinguishable in the observed dynamics, which typically leads to memory [15, 26, 47, 62–65]. For any *observable* transition between different observable states $j \rightarrow i$ with a preceding history sequence of length k , we denote the observed sequence as $\{s_t\}_{1 \leq t \leq k+2} = s_1 s_2 \cdots s_k j i$, and define the history sequence as $S_k \equiv \{s_t\}_{1 \leq t \leq k} = s_1 s_2 \cdots s_k$. [66] A corresponding microscopic (fully resolved) sequence is denoted by $\{\sigma_\tau\}_{1 \leq \tau \leq k'} = \sigma_1 \sigma_2 \cdots$. The length of a microscopic sequence corresponding to $\{s_t\}_{1 \leq t \leq k+2}$ is $k' \geq k+2$ but may become arbitrarily long, as some microscopic transitions may not change observable states and thus are not seen in the observed time series.

We further define a reduced sequence of microscopic states $\{\alpha_t\}_{1 \leq t \leq k+2}$ consisting of only the first microscopic step after every observable transition as $\alpha_t = \sigma_{\tau(t)}$, where $\tau(1) = 1$, and $\tau(t+1) = \inf\{\tau' : \tau' > \tau(t), \mathbb{1}_{s_{t+1}}[\sigma_{\tau'}] = 1\}$ for any $t \geq 1$. In other words, we construct the reduced sequence by revealing the first microscopic state in every observable step, as illustrated in FIG. (1). [67] The dynamics of the reduced microscopic sequence $\{\alpha_t\}_{1 \leq t \leq k+2}$ is Markov. The microscopic transition probability is given by an effective transition matrix Ω , whose elements are transition probabilities $\Omega_{\alpha_{t+1}\alpha_t} = \mathbb{P}(\alpha_{t+1}|\alpha_t)$ (See derivation in the Supplementary Material [68]). The sequence probability is given by $\mathbb{P}(\{\alpha_t\}_{1 \leq t \leq k}) = \prod_{i=t}^{k-1} \mathbb{P}(\alpha_{t+1}|\alpha_t)\mathbb{P}(\alpha_1)$, where $\mathbb{P}(\alpha_1)$ is the steady state probability at α_1 in the reduced sequence.



FIG. 1. (a) A schematic illustrating the definition of a microscopic full sequence $\{\sigma_\tau\}_{1 \leq \tau \leq k'}$ (above), a reduced sequence $\{\alpha_t\}_{1 \leq t \leq k+2}$ (middle), and the observable sequence $\{s_t\}_{1 \leq t \leq k+2}$ (below).

Distribution of histories.—For any pair of observed states j and i , we denote the probability of the sequence $S_k \rightarrow j \rightarrow i$ by $\mathbb{P}(ijS_k)$. Let $\{S_k^j\} \subset \{S_k\}$ be the countable set of possible (distinct) histories with length k that precede j , which is a subset of all possible sequences with

length k . We introduce a shorthand notation for the sum of probabilities of microscopic sequences with the same observable history S_k^j as

$$\mathbb{P}(\alpha_{k+1}S_k^j) \equiv \sum_{\{\alpha_t\}_{1 \leq t \leq k}} \mathbb{1}_{S_k^j}[\{\alpha_t\}_{1 \leq t \leq k}] \mathbb{P}(\{\alpha_t\}_{1 \leq t \leq k+1}), \quad (1)$$

where $\mathbb{1}_X$ is the indicator function of the set X , taking the value 1 if the microscopic sequence $\{\alpha_t\}_{1 \leq t \leq k}$ is projected onto the observable sequence S_k^j and 0 otherwise. The (generally non-Markovian) transition probability $j \rightarrow i$ conditioned on a specific history S_k^j is given by

$$\mathbb{P}(i|jS_k^j) = \frac{\sum_{\alpha_{k+1}} \mathbb{1}_j[\alpha_{k+1}] \mathbb{P}(\alpha_{k+1}S_k^j) \mathbb{P}(i|\alpha_{k+1})}{\sum_{\alpha_{k+1}} \mathbb{1}_j[\alpha_{k+1}] \mathbb{P}(\alpha_{k+1}S_k^j)}, \quad (2)$$

where $\mathbb{P}(i|\alpha_{k+1}) \equiv \sum_{\alpha_{k+2}} \mathbb{1}_i[\alpha_{k+2}] \mathbb{P}(\alpha_{k+2}|\alpha_{k+1})$. By definition, the observed sequence is Markov *if and only if* the transition probability between any pair of states does *not* depend on the history. However, Eq. (2) shows that the observed transition probability $j \rightarrow i$ is a weighted average of microscopic splitting probabilities from α_{k+1} to α_{k+2} , and the weights $\mathbb{P}(\alpha_{k+1}S_k^j)$ depend on the history. Since different history sequences S_k^j impose different weights and yield different conditional probabilities $\mathbb{P}(i|jS_k^j)$, we may use histograms of $\mathbb{P}(i|jS_k^j)$ to infer memory systematically and, by the explicit dependence on i and j , locally. The dynamics of the observed sequence is Markov *if and only if* for any pair i, j and for any k all histograms $\mathbb{P}(i|jS_k^j)$ are Kronecker delta distributions, i.e. display a single bar at $\mathbb{P}(i|jS_k^j) = \mathbb{P}(i|j)$. If there exist certain j and i where the histogram at some k has non-zero values at locations other than $\mathbb{P}(i|j)$, then the transition from j to i has memory, and therefore the state j is non-Markov.

We create a histogram for $\{S_k^j\}$ by binning $\mathbb{P}(i|jS_k^j)$ as

$$h_k^\delta(p) \equiv \frac{1}{\mathbb{P}(j)} \sum_{\{S_k^j\}} \mathbb{P}(jS_k^j) \mathbb{1}_{[p-\delta, p+\delta]}[\mathbb{P}(i|jS_k^j)], \quad (3)$$

such that those S_k^j giving the value of conditional probabilities satisfying $\mathbb{P}(i|jS_k^j) \in [p-\delta, p+\delta]$ are classified into the same bar. Each S_k^j is weighted by the sequence probability $\mathbb{P}(jS_k^j)$, with a normalization factor $\mathbb{P}(j)$. It is easy to see from Eq. (2) that the positions of non-zero bars are bounded by the smallest and largest values of $\mathbb{P}(\alpha_{t+1}|\alpha_t)$ (see [68], Sec. I).

Convergence of histograms.—By comparing histograms for different history length k , we can obtain information on the duration of *local memory*. Changes in the histograms upon increasing k reflect the memory about the past. If a conditioned histogram for the transition $i \rightarrow j$ converges to a stationary distribution at some $k \geq n$, then the system only remembers up to n steps in the past prior to the transition. The hidden microscopic paths projecting onto the states observed $k \geq n$

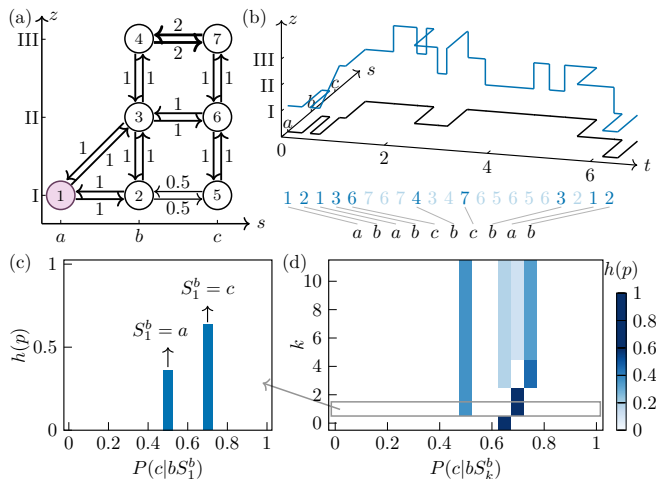


FIG. 2. (a) A schematic of the full Markov network. s -axis is the observable dimension and z -axis is the hidden dimension. Microscopic states 2, 3, 4 and 5, 6, 7 are lumped into observable states b and c , respectively. State a is an observable Markov state, as it corresponds to a single microscopic state 1. The numbers on arrows are the transition rates for the Markov jump process. (b) The upper panel is an example of a microscopic trajectory in blue and the observed trajectory in black. The observed trajectory is a projection of the microscopic trajectory onto the s - t plane. The lower panel shows the corresponding full microscopic sequence (top), including the sequence of first steps after each observable transition in solid color, and the observed sequence (bottom). (c) The histogram for the transition probability from state b to c conditioned on one step in the history $P(c|bS_1^b)$, where $\{S_1^b\} = \{a, c\}$. The two bars are contributed from $P(c|ba)$ and $P(c|bc)$. (d) A kymograph of histograms for $P(c|bS_k^b)$ with different lengths of history k .

steps in the past thus mix in path space prior to the observed transition $i \rightarrow j$, which erases memory about the more distant past. The convergence rate of the histograms therefore informs about the temporal extent of *local memory*.

We prove the convergence of the histograms under the assumption that there is at least one “observable Markov state” γ in the network, while we do not need to know which state it is exactly. This is sufficient but not necessary for convergence [69]. An “observable Markov state” γ is an observed state corresponding to only one microscopic state (i.e., no hidden states corresponding to this observable state), satisfying the Markov property: for any integers $k \geq 1$ and $g \geq k + 2$, for any future sequence $\{s_t\}_{k+2 \leq t \leq g}$ and history sequence $\{s_t\}_{1 \leq t \leq k}$,

$$\begin{aligned} & \mathbb{P}(\{s_t\}_{k+2 \leq t \leq g} | s_{k+1} = \gamma; \{s_t\}_{1 \leq t \leq k}) \\ &= \mathbb{P}(\{s_t\}_{k+2 \leq t \leq g} | s_{k+1} = \gamma). \end{aligned} \quad (4)$$

To formalize the convergence of histograms we introduce the transition matrix Ψ , such that the observable Markov state γ is an absorbing state, and other transition probabilities the same as in Ω . We prove that the total variation distance (TVD) between the histogram \mathbf{h}_k and the

“stationary” histogram \mathbf{h}_∞ is bounded by

$$\|\mathbf{h}_k - \mathbf{h}_\infty\|_{\text{TV}} \leq C|\lambda_1|^k, \quad (5)$$

where λ_1 is the eigenvalue of Ψ with the second largest modulus, and C is a constant depending on Ω . See a sketch of proof in Appendix A and the detailed proof in [68]. Specifically, if the observed sequence is an n -th (definite) order Markov process, then there exists an n , for any $k \geq n$ and any S_k^j , $\mathbb{P}(i|jS_k^j) = \mathbb{P}(i|jS_n^j)$. In this case the histograms fully converge for $k \geq n$.

We now briefly discuss the concept of an n -th order Markov process, meaning that the future events are fully decided by n steps in the past. Convergence of histograms suggests that we can also consider a “weaker” definition of an n -th order Markov process, where all the histograms for S_n approach stationary distributions, i.e. changes become sufficiently small for $k > n$. In most realistic scenarios one encounters weak n -th order Markov processes.

Notably, the concept of “Markovian events”—events whose detection implies conditional independence between past and future time evolution—was proposed in [50, 59, 60]. The assumption that such events can be identified turns out to provide a crucial improvement in thermodynamic inference. However, so far Eq. (4) could not be generally tested in practice, as it is impossible to test for arbitrarily large g and k with a finite trajectory. Note that the Markov property at a specific state for a one-step transition $\mathbb{P}(s_{g+1}|s_g = \gamma; \{s_t\}_{1 \leq t \leq g-1}) = \mathbb{P}(s_{g+1}|s_g = \gamma)$ is only a necessary but *not* sufficient condition for the Markov property. Here we provide a new tool to further test for a Markov state, though it is still not a complete solution. In the case of observable dynamics with a *definite* order n , it is sufficient to test the Markovianity for no more than n steps in the past and in the future (see [68] for details), which is practically feasible. Moreover, one can test for more than one first step in the future to get a more reliable (though still not definite) detection of a Markov state. Considering such extended future sequences also provides more information on the microscopic network (see Appendix B for details).

Example.—Consider the 7-state Markov network in Fig. 2. The eigenvalues of the corresponding splitting-probability matrix Φ , of the effective transition matrix Ω , and of that obtained by setting the observable Markov state as an absorbing state are shown in Table I.

TABLE I. Eigenvalues of the splitting probability matrix Φ , the effective transition matrix Ω , and the transition matrix Ψ with absorbing boundary at state a .

	λ_0	λ_1	λ_2	λ_3	λ_4	λ_5	λ_6
Φ	1	-0.923	0.639	-0.557	0.374	-0.369	-0.164
Ω	1	-1	0.635	-0.635	0.199	-0.199	0
Ψ	1	0.861	-0.861	0.405	-0.405	0.193	-0.193

Kymographs of transition probabilities $\mathbb{P}(i|jS_k^j)$ be-

tween different pairs of states conditioned on histories are shown in Fig. 3(a-c). Specifically, the conditional probability $\mathbb{P}(b|aS_k^a)$ and $\mathbb{P}(b|cS_k^c)$ in panel (a) take the value 1 independent of the histories, because states a and c are reflecting.

We first look at the histogram of $\mathbb{P}(c|bS_k^b)$ with only two bars in Fig. 2(c), which corresponds to one row in the kymograph for $\mathbb{P}(c|bS_k^b)$. The number of bars in the histogram of $\mathbb{P}(i|jS_1^j)$ is constrained by the number of states directly connected to j , i.e. the number of possible histories S_1 . As the history sequence S_k^j becomes longer, the histograms include more information about the history, and more bars at different positions appear. When the history length k becomes sufficiently large, the histogram converges to a stationary distribution. The dynamics of the observed sequence in Fig. (2) and (3) can be considered a *locally* 5-th order Markov process in the weak sense of convergence with cutoff $\|\mathbf{h}_k - \mathbf{h}_\infty\| < 10^{-4}$ for any $k \geq 5$.

A comparison between the TVD from simulation and the theoretical bound is shown in Fig. 3(d). The TVD from simulation is determined by $\|\mathbf{h}_k - \mathbf{h}_{k_{\max}}\|_{\text{TV}} \leq 2\|\mathbf{h}_k - \mathbf{h}_\infty\|_{\text{TV}}$. In agreement with Eq. (5), the histograms converge to stationary histograms for large k . While the actual convergence is faster than the theoretical bound (i.e. the bound is loose), the theory is verified.

Discussion.—A first application of the method is to test the consistency of Markov-state models. It is common to model single-molecule trajectories with a Markov transition network [5, 70]. For fitted trajectories, we can build histograms for the transition probabilities conditioned on different lengths of history. If a Markov model indeed captures all relevant states, i.e. does not leave any hidden paths between observed states, then histograms between any pair of states should display a single bar which remains the same for any history length. If the trajectories are not long enough, or their number is not large enough, the probability distributions in the histograms may evolve (i.e. spread) as the history length increases due to undersampling, while the distribution should concentrate around the same value. However, if the histograms for a specific pair of states exhibit more than one peak that changes with the history length, this *conclusively* implies hidden paths between said pair of states that are *not* captured in the Markov model.

Moreover, since observed transition probabilities are always linear combinations of effective microscopic transition probabilities $\mathbb{P}(\alpha_{k+2}|\alpha_{k+1})$, as shown in Eq. (2), the locations of bars are always within the range of the minimum and maximum of the effective microscopic transition probabilities. Based on this property, the histograms also provide information on the range of effective hidden transition probabilities. Therefore, the locations of bars in histograms provide information on hidden transition probabilities between a given pair of states, and the convergence of the respective histograms reveals the extent of memory *locally*.

Conclusion.—In this Letter, we proposed a histogram-

based method to infer, for the first time, memory *locally*, i.e. non-Markovianity of transitions between any pair of observed states. The method is based on transition probabilities conditioned on history sequences of different lengths. The convergence rate of these “history” histograms towards a stationary distribution provides, for the first time, a *local quantification of the duration of memory*, which reflects how distinct microscopic paths projecting onto the same observed transition decorrelate in path space. Accordingly, this provides information about the hidden topology of microscopic paths in a holography-like fashion. Under the assumption of at least one observable Markov state, we proved that the histograms indeed always converge to a stationary distribution when the history becomes infinitely long. The analytical predictions were corroborated by simulation results for a 7-state Markov network example.

The histogram-based method provides information on local (hidden) properties of the network, which is quite different from (but complementary to) the information gained from local waiting time distributions. The method may be easily extended to account for waiting times, by simply discretizing the continuous-time trajectory with a fixed time interval. However, the statistics would depend on the discretization. In practice, the analysis of discretized continuous-time trajectories requires longer trajectories for sufficient sampling than the analysis of sequences eliminating waiting times. The method can be applied to test whether a Markov-state model consistently captures the underlying dynamics and also provides a more reliable (yet still *not* definitive) practical criterion for a “Markov state”. It would be interesting to connect the local memory inferred here to properties of memory kernels [28–32, 36, 37] and to seek for a holography-like understanding of the weak-memory regime [34, 35].

Acknowledgments.—Financial support from the Volkswagen Stiftung together with the Ministry of Science and Culture of the German State of Lower Saxony within the scope of the “Research Cooperation Lower Saxony - Israel” (to A.G.), the European Research Council (ERC) under the European Union’s Horizon Europe research and innovation program (Grant Agreement No. 101086182 to A.G.), the US National Science Foundation (Grant no. CHE 2400424 to DEM), the Robert A. Welch Foundation (Grant no. F-1514 to D.E.M.) and the Alexander von Humboldt Foundation is gratefully acknowledged.

Appendix A: Sketch of proof of the convergence of histograms.—To prove the convergence of histograms, we split all possible history sequences S_k^j into two disjoint sets depending on whether they have visited the observable Markov state γ in the history of k steps ($\{S_k^j\}^M$) or not ($\{S_k^j\}^N$). The histogram is also decomposed into two parts, $h_k(p) = h_k^M(p) + h_k^N(p)$.

We define the history extended further into the past to be $S_{k+l} \equiv \{s_t\}_{-l+1 \leq t \leq k}$, $l \geq 1$, and $\{S_{k+l}\}^M$ as the trajectories that do *not* visit γ in the last k steps during

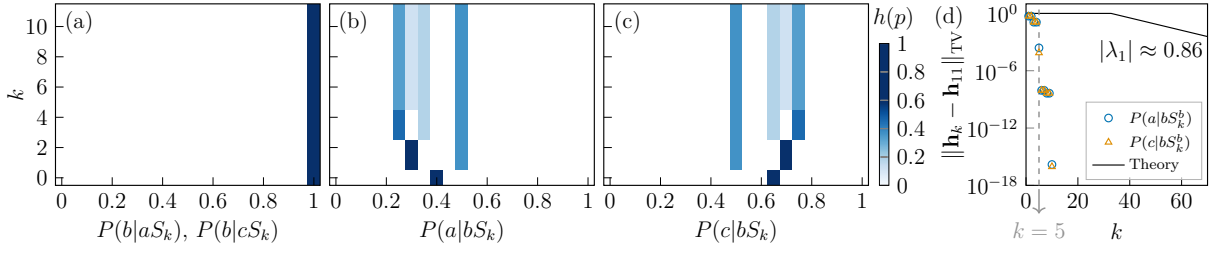


FIG. 3. (a)-(c) Kymographs of histograms of transition probabilities between different pairs of states conditioned on history of length k . Each row represents a histogram for a fixed history length k . The color bar is the same for all kymographs. (d) The points show the TVD determined from simulation results, and the line is the theoretical bound which is independent of the pair of states. The gray dashed line at $k = 5$ denotes the border beyond which the TVD is smaller than a convergence cutoff 10^{-4} .

$\{s_t\}_{1 \leq t \leq k}$. We can show that the contribution from $S_k^j \in \{S_k^j\}^M$ to the histogram $h(p)$ is the same as that from $\{S_{k+l}^j\}^M$, because the dynamics is always “renewed” after visiting the observable Markov state and therefore does *not* depend on the earlier history.

By utilizing the convergence theorem of a Markov chain to a stationary distribution, we can prove that the contribution from $S_k^j \in \{S_k^j\}^N$ is bounded by

$$\sum_{n=0}^L h_k^N(p = 2n\delta) \leq C |\lambda_1|^{k+1-m^*} \binom{k+1}{m^*-1}, \quad (\text{A.6})$$

where λ_1 is the eigenvalue of the transition matrix Ψ with the second largest modulus, C is a constant determined by the transition matrix, and m^* is the dimension of the largest Jordan block among all generalized eigenvalues of Ψ . For a fixed k , the contribution from $\{S_{k+l}^j\}^M$ is independent of l , and that from $\{S_{k+l}^j\}^N$ still changes with l but vanishes as l tends to infinity. A detailed proof is given in [68].

Appendix B: Conditional probability for the second step in the future.—We first state a sufficient condition where for some j and i , for any k , $\mathbb{P}(i|jS_k^j)$ is a delta distribution, i.e. Eq. (2) is independent of S_k^j : $\mathbb{P}(i|\alpha_{k+1})$ are the same for any α_{k+1} in j . An example for the dynamics for reduced sequences satisfying this condition, which yields $\mathbb{P}(i|jS_k^j) = p$ independent of the history, is shown in Fig. (4). Another example satisfying the condition can be found in [71].

Now suppose that for some observable state j , for any i directly connected to j and any k , all the histograms show delta distributions at the same location $\mathbb{P}(i|j)$. The transition from j to one step in the future does not display memory. In this case, state j may be, but not necessarily is, a Markov state. Nonetheless, we can check the conditional probability of arriving at state o at the $(k+3)$ -th step conditioned on being at j at the $(k+1)$ -th

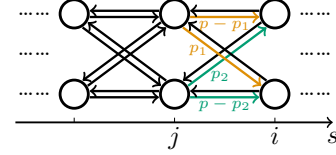


FIG. 4. A part of a network for the dynamics of the reduced microscopic sequence. The values on arrows represent elements in the transition matrix Ω for the reduced sequence. The two microscopic states in the observable state j both satisfy $\mathbb{P}(i|\alpha_{k+1}) = p$.

step with a history S_k , as

$$\mathbb{P}(s_{k+3} = o|s_{k+1} = j; S_k) = \frac{\sum_{\alpha_{k+1}} \mathbb{1}_j[\alpha_{k+1}] \mathbb{P}(\alpha_{k+1} S_k^j) \sum_{\alpha_{k+2}} \mathbb{P}(o|\alpha_{k+2}) \mathbb{P}(\alpha_{k+2}|\alpha_{k+1})}{\sum_{\alpha_{k+1}} \mathbb{1}_j[\alpha_{k+1}] \mathbb{P}(\alpha_{k+1} S_k^j)}, \quad (\text{A.7})$$

where $\mathbb{P}(o|\alpha_{k+2}) = \sum_{\alpha_{k+3}} \mathbb{1}_o[\alpha_{k+3}] \mathbb{P}(\alpha_{k+3}|\alpha_{k+2})$. Note that o is a second-order neighbor of j in the connectivity graph. If the histograms for $\mathbb{P}(s_{k+3} = o|s_{k+1} = j; S_k)$ depend on S_k , i.e. are *not* delta distributions at the same location, then state j is in fact non-Markov.

If some histograms for $\mathbb{P}(s_{k+3} = o|s_{k+1} = j; S_k)$ are not delta distributions, we can also tell, from Eq. (A.7), that the sums $\sum_{\alpha_{k+2}} \mathbb{P}(o|\alpha_{k+2}) \mathbb{P}(\alpha_{k+2}|\alpha_{k+1}) = \mathbb{P}(s_{k+3} = o|\alpha_{k+1})$ are not the same for all the α_{k+1} in state j . The contrapositive statement can easily be shown by assuming the sum $\mathbb{P}(s_{k+3} = o|\alpha_{k+1})$ is a constant for any α_{k+1} . Then, the summation over α_{k+1} in Eq. (A.7) cancels. Furthermore, the dependence of $\mathbb{P}(s_{k+3} = o|\alpha_{k+1})$ on α_{k+1} means that $\mathbb{P}(o|\alpha_{k+2})$ are not the same for all the α_{k+2} directly connected to any microscopic states in j . Otherwise, we have that $\mathbb{P}(s_{k+3} = o|\alpha_{k+1}) = \mathbb{P}(o|\alpha_{k+2}) \sum_{\alpha_{k+2}} \mathbb{P}(\alpha_{k+2}|\alpha_{k+1}) = \mathbb{P}(o|\alpha_{k+2})$ does *not* depend on α_{k+1} , which contradicts the first statement. Note that all the statements here are uni-directional. The statements above show that investigating memory locally yields information on microscopic transition probabilities, even though memory

is determined by the entire network.

Similarly, we can always check for any step further in the future $\mathbb{P}(s_{k+\Delta} = o | s_{k+1} = j; S_k)$ ($\Delta \geq 2$) to be more “certain” about state j being a Markov state, while it

is generally *not* practically feasibly (for obvious reasons) to check the probabilities of arbitrary future sequences conditioned on histories.

-
- [1] G. A. Papoian and P. G. Wolynes, *Biopolymers* **68**, 333 (2003).
- [2] D. J. Wales, *Annu. Rev. Phys. Chem.* **69**, 401–425 (2018).
- [3] J. C. Schön, *J. Chem. Phys.* **161**, 050901 (2024).
- [4] B. K. Chu, M. J. Tse, R. R. Sato, and E. L. Read, *BMC Syst. Biol.* **11**, 1 (2017).
- [5] D. Shukla, C. X. Hernández, J. K. Weber, and V. S. Pande, *Acc. Chem. Res.* **48**, 414 (2015).
- [6] S. Shafiekhani, P. Kraikivski, N. Gheibi, M. Ahmadian, and A. H. Jafari, *Curr. Genet.* **67**, 785–797 (2021).
- [7] S. S. Plotkin and P. G. Wolynes, *Phys. Rev. Lett.* **80**, 5015 (1998).
- [8] W. C. Swope, J. W. Pitera, and F. Suits, *J. Phys. Chem. B* **108**, 6571 (2004).
- [9] W. Min, *Phys. Rev. Lett.* **94**, 198302 (2005).
- [10] F. Noé and S. Fischer, *Curr. Opin. Struct. Biol.* **18**, 154 (2008).
- [11] A. K. Sangha and T. Keyes, *J. Phys. Chem. B* **113**, 15886 (2009).
- [12] J. Stigler, F. Ziegler, A. Gieseke, J. C. M. Gebhardt, and M. Rief, *Science* **334**, 512 (2011).
- [13] N. Narinder, C. Bechinger, and J. R. Gomez-Solano, *Phys. Rev. Lett.* **121**, 078003 (2018).
- [14] A. G. T. Pyo and M. T. Woodside, *Phys. Chem. Chem. Phys.* **21**, 24527 (2019).
- [15] L. Vollmar, R. Bebon, J. Schimpf, B. Flietel, S. Celiksoy, C. Soennichsen, A. Godec, and T. Hugel, *J. Phys. Math. Theor.* **57**, 365001 (2024).
- [16] I. Di Terlizzi, F. Ritort, and M. Baiesi, *J. Stat. Phys.* **181**, 1609–1635 (2020).
- [17] I. D. Terlizzi and M. Baiesi, *J. Phys. A: Math. Theor.* **53**, 474002 (2020).
- [18] M. Baiesi, T. Nishiyama, and G. Falasco, *Commun. Phys.* **7**, 10.1038/s42005-024-01742-2 (2024).
- [19] R. Zwanzig, *J. Chem. Phys.* **33**, 1338 (1960).
- [20] H. Mori, *Progr. Theoret. Phys. Suppl.* **33**, 423 (1965).
- [21] H. Haken, *Rev. Modern Phys.* **47**, 67 (1975).
- [22] R. Zwanzig, *Nonequilibrium Statistical Mechanics* (Oxford University Press, 2001).
- [23] D. E. Makarov, *J. Chem. Phys.* **138**, 014102 (2013).
- [24] S. M. Avdoshenko, A. Das, R. Satija, G. A. Papoian, and D. E. Makarov, *Sci. Rep.* **7**, 269 (2017).
- [25] M. Ozmaian and D. E. Makarov, *J. Chem. Phys.* **151**, 235101 (2019).
- [26] A. Lapolla and A. Godec, *Front. Phys.* **7**, 182 (2019).
- [27] C. Ayaz, L. Scalfi, B. A. Dalton, and R. R. Netz, *Phys. Rev. E* **105**, 054138 (2022).
- [28] T. Schilling, *Phys. Rep.* **972**, 1 (2022).
- [29] F. Ginot, J. Caspers, M. Krüger, and C. Bechinger, *Phys. Rev. Lett.* **128**, 028001 (2022).
- [30] A. Abbasi, R. R. Netz, and A. Najji, *Phys. Rev. Lett.* **131**, 228202 (2023).
- [31] L. Lavacchi and R. R. Netz, *J. Chem. Phys.* **161**, 10.1063/5.0225742 (2024).
- [32] B. A. Dalton, A. Klimek, H. Kiefer, F. N. Brünig, H. Colinet, L. Tepper, A. Abbasi, and R. R. Netz, *Annu. Rev. Phys. Chem.* **10.1146/annurev-physchem-082423-031037** (2025).
- [33] K. Engbring, D. Boriskovsky, Y. Roichman, and B. Lindner, *Phys. Rev. X* **13**, 021034 (2023).
- [34] K. Brandner, *Phys. Rev. Lett.* **134**, 037101 (2025).
- [35] K. Brandner, *Phys. Rev. E* **111**, 014137 (2025).
- [36] C. Widder, F. Koch, and T. Schilling, *J. Chem. Phys.* **157**, 194107 (2022).
- [37] T. Schilling, *J. Chem. Phys.* **161**, 191501 (2024).
- [38] D. R. Westhead, M. Vijayabaskar, and M. Westhead, *Hidden Markov Models: Methods and Protocols* (Springer New York, 2017).
- [39] T. Hastie, R. Tibshirani, and J. Friedman, *The Elements of Statistical Learning* (Springer New York, 2009).
- [40] D. L. Weakliem, *Sociol. Methods Res.* **27**, 359 (1999).
- [41] B. Liseo, Robustness issues in bayesian model selection, in *Robust Bayesian Analysis* (Springer New York, 2000) p. 197–222.
- [42] A. M. Berezhkovskii and D. E. Makarov, *J. Phys. Chem. Lett.* **9**, 2190 (2018).
- [43] R. Satija, A. M. Berezhkovskii, and D. E. Makarov, *Proc. Natl. Acad. Sci.* **117**, 27116 (2020).
- [44] D. Hartich and A. Godec, *Phys. Rev. X* **11**, 041047 (2021).
- [45] A. Lapolla and A. Godec, *Phys. Rev. Res.* **3**, L022018 (2021).
- [46] K. Song, D. E. Makarov, and E. Vouga, *Phys. Rev. Res.* **5**, L012026 (2023).
- [47] X. Zhao, D. Hartich, and A. Godec, *Phys. Rev. Lett.* **132**, 147101 (2024).
- [48] D. S. Talaga, *Curr. Opin. Colloid Interface Sci.* **12**, 285 (2007).
- [49] P. V. Cornish, D. N. Ermolenko, H. F. Noller, and T. Ha, *Mol. Cell* **30**, 578 (2008).
- [50] J. Degünther, J. van der Meer, and U. Seifert, *Proc. Natl. Acad. Sci.* **121**, e2405371121 (2024).
- [51] D. Hartich and A. Godec, *Nat. Commun.* **15**, 8678 (2024).
- [52] J. Mehl, B. Lander, C. Bechinger, V. Blickle, and U. Seifert, *Phys. Rev. Lett.* **108**, 220601 (2012).
- [53] É. Roldán and J. M. R. Parrondo, *Phys. Rev. Lett.* **105**, 150607 (2010).
- [54] É. Roldán and J. M. R. Parrondo, *Phys. Rev. E* **85**, 031129 (2012).
- [55] U. Seifert, *Rep. Progr. Phys.* **75**, 126001 (2012).
- [56] M. Esposito, *Phys. Rev. E* **85**, 041125 (2012).
- [57] P. E. Harunari, A. Dutta, M. Poletti, and É. Roldán, *Phys. Rev. X* **12**, 041026 (2022).
- [58] J. van der Meer, B. Ertel, and U. Seifert, *Phys. Rev. X* **12**, 031025 (2022).
- [59] J. van der Meer, J. Degünther, and U. Seifert, *Phys. Rev. Lett.* **130**, 257101 (2023).
- [60] J. Degünther, J. van der Meer, and U. Seifert, *Phys. Rev. Res.* **6**, 023175 (2024).

- [61] K. Blom, K. Song, E. Vouga, A. Godec, and D. E. Makarov, *Proc. Natl. Acad. Sci.* **121**, e2318333121 (2024).
- [62] C. Dieball and A. Godec, *J. Chem. Phys.* **162**, 090901 (2025).
- [63] T. Schwarz, A. B. Kolomeisky, and A. Godec, [arXiv:2410.11819](https://arxiv.org/abs/2410.11819) (2024).
- [64] A. Godec and D. E. Makarov, *J. Phys. Chem. Lett.* **14**, 49 (2023).
- [65] D. Hartich and A. Godec, *Phys. Rev. Res.* **5**, L032017 (2023).
- [66] Note that the states visited in any pair of consecutive steps are distinct, i.e. $\forall t, s_t \neq s_{t+1}$.
- [67] Generally, different $\{\alpha_t\}_{1 \leq t \leq k+2}$ can yield the same $\{s_t\}_{1 \leq t \leq k+2}$.
- [68] See Supplemental Material at [...] for the calculation of the new transition matrix, discussion on detection of Markov state, and the proof of the convergence of histograms, as well as Refs. [50, 59, 60, 72–75].
- [69] There are systems that violate the assumption but still yield converging histograms.
- [70] J. D. Chodera and F. Noé, *Curr. Opin. Struct. Biol.* **25**, 135 (2014).
- [71] O. A. Igoshin, A. B. Kolomeisky, and D. E. Makarov, *J. Chem. Phys.* **162**, 034111 (2025).
- [72] K. R. Garren, *Bounds for the Eigenvalues of a Matrix*, Vol. 4373 (National Aeronautics and Space Administration, 1968).
- [73] J. S. Rosenthal, *SIAM Rev.* **37**, 387 (1995).
- [74] T. M. Silva, L. Silva, and S. Fernandes, *Linear Algebra Appl.* **488**, 199 (2016).
- [75] H. Robbins, *Amer. Math. Monthly* **62**, 26 (1955).

Supplementary Material for: Towards Markov-State Holography

Xizhu Zhao¹, Dmitrii E. Makarov^{2, 3}, and Aljaž Godec¹

¹*Mathematical bioPhysics Group, Max Planck Institute for Multidisciplinary Sciences, Am Fassberg 11, 37077 Göttingen, Germany*

²*Department of Chemistry, University of Texas at Austin, Austin, Texas 78712, USA*

³*Oden Institute for Computational Engineering and Sciences, University of Texas at Austin, Austin, Texas 78712, USA*

In this Supplementary Material (SM), we present details of calculations and mathematical proofs.

CONTENTS

S1. Effective transition matrix	1
S2. Detection of observable Markov state	3
S3. Convergence of histograms	4
1. Contribution from trajectories that visited the Markov state	4
2. Contribution from trajectories that did not visit the Markov state	5
References	7

Appendix S1: Effective transition matrix

In this section we introduce an effective transition matrix Ω for the reduced sequence $\{\alpha_t\}_{1 \leq t \leq k+2}$ consisting of the first microscopic steps after each observable transition. In the main text, we defined the observed sequence $\{s_t\}_{1 \leq t \leq k+2}$ and a corresponding microscopic (fully resolved) sequence $\{\sigma_\tau\}_{1 \leq \tau \leq k'}$ ($k' \geq k+2$).

Assume that the system has m microscopic states $\{1, \dots, m\}$ which are projected onto n observable states $\{1, \dots, n\}$. The microscopic states are enumerated in an order such that those projected onto the same observable state are adjacent. We denote the number of microscopic states in an observable state a as r_a , satisfying $\sum_{a=1}^n r_a = m$.

As an example we first consider a one-step transition. Assume the current microscopic state α_t is projected to an observable state $s_t = s$. We define for short that $g \equiv \sum_{a=1}^{s-1} r_a$ and $r \equiv r_s$, i.e. the observable state s consists of r microscopic states. We partition the transition probability matrix Φ into block matrices by separating the columns corresponding to the observable state s , as

$$\Phi = \begin{pmatrix} \boxed{\Phi_{11}^{g \times g}} & \mathbf{R}^{g \times r} & \boxed{\Phi_{13}^{(g+r) \times (m-g-r)}} \\ \boxed{\Phi_{31}^{(m-g) \times g}} & \mathbf{Q}^{r \times r} & \boxed{\Phi_{33}^{(m-g-r) \times (m-g-r)}} \end{pmatrix}, \quad (\text{S1})$$

where the superscripts indicate the dimensions of the respective block matrices. Since we do *not* distinguish the microscopic full sequences which stay in the observable state s for arbitrary steps before jumping to another observable state, we consider the sum of the probabilities of all microscopic sequences $\{\sigma_\tau\}_{\tau(t)+1 \leq \tau' \leq \tau(t+1)-1}$ which stay in the observable state s_t until the next observable step $t+1$. Therefore, the transition probability $\Omega_{\alpha_{t+1}|\alpha_t} = \mathbb{P}(\alpha_{t+1}|\alpha_t)$ for the reduced sequence given by

$$\begin{aligned} \mathbb{P}(\alpha_{t+1}|\alpha_t) &= \sum_{\tau(t+1)=\tau(t)+1}^{\infty} \sum_{\{\sigma_\tau\}_{\tau(t)+1 \leq \tau' \leq \tau(t+1)-1}} \mathbb{P}(\sigma_{\tau(t+1)} = \alpha_{t+1}; \{\sigma_{\tau'}\}_{\tau(t)+1 \leq \tau' \leq \tau(t+1)-1} | \sigma_{\tau(t)} = \alpha_t) \\ &= \sum_{\tau(t+1)=\tau(t)+1}^{\infty} \sum_{\sigma_{\tau(t)+1}=g+1}^{g+r} \sum_{\sigma_{\tau(t)+2}=g+1}^{g+r} \cdots \sum_{\sigma_{\tau(t+1)-1}=g+1}^{g+r} \underbrace{\Phi_{\alpha_{t+1}\sigma_{\tau(t+1)-1}}}_{\begin{pmatrix} \mathbf{R} \\ \mathbf{0} \\ \mathbf{R}' \end{pmatrix}} \underbrace{\prod_{\tau'=\tau(t)}^{\tau(t+1)-2} \Phi_{\sigma_{\tau'+1}\sigma_{\tau'}}}_{\mathbf{Q}^{\tau(t+1)-\tau(t)-1}}. \end{aligned} \quad (\text{S2})$$

Note that when $\tau(t+1) = \tau(t) + 1$, there is no summation or product, i.e. the first term is given by $\Phi_{\alpha_{t+1}\alpha_t} \mathbb{P}(\alpha_t)$. For example, if we consider $t = 1$, then $\tau(1) = 1$, and Eq. (S2) becomes

$$\Phi_{\alpha_2\alpha_1} \mathbb{P}(\alpha_1) + \sum_{\tau(2)=3}^{\infty} \sum_{\sigma_2=g+1}^{g+r} \cdots \sum_{\sigma_{\tau(2)-1}=g+1}^{g+r} \Phi_{\alpha_2\sigma_{\tau(2)-1}} \prod_{\tau'=2}^{\tau(2)-2} \Phi_{\sigma_{\tau'+1}\sigma_{\tau'}} \Phi_{\sigma_2\alpha_1} \mathbb{P}(\alpha_1). \quad (\text{S3})$$

With a change of variable $d \equiv \tau(t+1) - \tau(t) - 1$, Eq. (S2) can be written in the matrix formalism. For any $\alpha_{t+1} \in \{1, \dots, g\} \cup \{g+r+1, \dots, m\}$ and $\alpha_t \in \{g+1, \dots, g+r\}$,

$$\Omega_{\alpha_{t+1}\alpha_t} = \mathbb{P}(\alpha_{t+1}|\alpha_t) = \left(\begin{pmatrix} \mathbf{R} \\ \mathbf{0} \\ \mathbf{R}' \end{pmatrix} \sum_{d=0}^{\infty} \mathbf{Q}^d \right)_{\alpha_{t+1}\alpha_t} = \left(\begin{pmatrix} \mathbf{R} \\ \mathbf{0} \\ \mathbf{R}' \end{pmatrix} (\mathbf{I} - \mathbf{Q})^{-1} \right)_{\alpha_{t+1}\alpha_t}. \quad (\text{S4})$$

We used the identity $\sum_{d=0}^{\infty} \mathbf{Q}^d = (\mathbf{I} - \mathbf{Q})^{-1}$. Matrix $\mathbf{I} - \mathbf{Q}$ is always invertible because \mathbf{Q} has a spectral radius less than 1. To determine all the elements in Ω , we introduce a matrix Λ_s by setting all the states other than the microscopic states in s to absorbing states, yielding in a transition matrix

$$\Lambda_s \equiv \begin{pmatrix} \mathbf{I}^{g \times g} & \mathbf{R}^{g \times r} & \mathbf{0}^{(g+r) \times (m-g-r)} \\ \mathbf{0}^{(m-g) \times g} & \mathbf{Q}^{r \times r} & \mathbf{0}^{(g+r) \times (m-g-r)} \\ \mathbf{R}'^{(m-g-r) \times r} & \mathbf{I}^{(m-g-r) \times (m-g-r)} & \mathbf{0}^{(m-g-r) \times (m-g-r)} \end{pmatrix}. \quad (\text{S5})$$

It is easy to show that the d -th power of the matrix Λ_s is given by

$$\Lambda_s^d = \begin{pmatrix} \mathbf{I}^{g \times g} & \mathbf{R}(\mathbf{I}^{r \times r} - \mathbf{Q})^{-1}(\mathbf{I}^{r \times r} - \mathbf{Q}^d) & \mathbf{0}^{(g+r) \times (m-g-r)} \\ \mathbf{0}^{(m-g) \times g} & \mathbf{Q}^d & \mathbf{0}^{(g+r) \times (m-g-r)} \\ \mathbf{R}'(\mathbf{I}^{r \times r} - \mathbf{Q})^{-1}(\mathbf{I}^{r \times r} - \mathbf{Q}^d) & \mathbf{I}^{(m-g-r) \times (m-g-r)} & \mathbf{0}^{(m-g-r) \times (m-g-r)} \end{pmatrix}. \quad (\text{S6})$$

Therefore, the infinite power of Λ_s is given by

$$\Lambda_s^\infty \equiv \lim_{d \rightarrow \infty} \Lambda_s^d = \begin{pmatrix} \mathbf{I}^{g \times g} & \mathbf{R}(\mathbf{I}^{r \times r} - \mathbf{Q})^{-1} & \mathbf{0}^{(g+r) \times (m-g-r)} \\ \mathbf{0}^{(m-g) \times g} & \mathbf{0}^{r \times r} & \mathbf{0}^{(g+r) \times (m-g-r)} \\ \mathbf{R}'(\mathbf{I}^{r \times r} - \mathbf{Q})^{-1} & \mathbf{I}^{(m-g-r) \times (m-g-r)} & \mathbf{0}^{(m-g-r) \times (m-g-r)} \end{pmatrix}, \quad (\text{S7})$$

which contains the transition probabilities from the microscopic states in the observable state s to other microscopic states, i.e. Eq. (S4) can be expressed from from Λ_s^∞ .

More formally, we define the matrix to select the first and the third column (row) of a 3×3 block matrix as

$$\mathbf{U}_s^{(m-r) \times m} \equiv \begin{pmatrix} \mathbf{I}^{g \times g} & \mathbf{0}^{g \times r} & \mathbf{0}^{g \times (m-g-r)} \\ \mathbf{0}^{(m-g-r) \times g} & \mathbf{0}^{(m-g-r) \times r} & \mathbf{I}^{(m-g-r) \times (m-g-r)} \end{pmatrix}, \quad (\text{S8})$$

and the matrix to select the second column (row) as

$$\mathbf{V}_s^{r \times m} \equiv (\mathbf{0}^{r \times g} \quad \mathbf{I}^{r \times r} \quad \mathbf{0}^{r \times (m-g-r)}). \quad (\text{S9})$$

Then we can formally express Λ_s defined in Eq. (S5) as

$$\Lambda_s = \mathbf{U}_s^\top \mathbf{U}_s + \mathbf{U}_s^\top \mathbf{R}_s \mathbf{V}_s + \mathbf{V}_s^\top \mathbf{Q}_s \mathbf{V}_s, \quad (\text{S10})$$

where $\mathbf{R}_s = \mathbf{U}_s \Phi \mathbf{V}_s^\top$, $\mathbf{Q}_s = \mathbf{V}_s \Phi \mathbf{V}_s^\top$. The sets of microscopic states projected onto different observable states are disjoint. Thus, we can carry out the same calculation for all $s \in \{1, \dots, n\}$ and define

$$\Lambda \equiv \sum_{s=1}^n (\mathbf{U}_s^\top \mathbf{R}_s \mathbf{V}_s + \mathbf{V}_s^\top \mathbf{Q}_s \mathbf{V}_s). \quad (\text{S11})$$

Therefore, the new ‘‘effective’’ transition matrix is given by the infinite power of Λ as

$$\Omega \equiv \Lambda^\infty = \sum_{s=1}^n \mathbf{U}_s^\top \mathbf{R}_s (\mathbf{I} - \mathbf{Q}_s)^{-1} \mathbf{V}_s. \quad (\text{S12})$$

Every column of Ω adds up to 1, and the diagonal blocks are all-zero matrices, agreeing with the fact that there is no “self-loop” in the observable sequence. Every block matrix corresponds to the microscopic transition probabilities between two observable states. We can write Ω more explicitly in block form as

$$\Omega = \begin{pmatrix} \mathbf{0}^{r_1 \times r_1} & \mathbf{R}_2(\mathbf{I}^{r_2 \times r_2} - \mathbf{Q}_2)^{-1} & \dots & \mathbf{R}_n(\mathbf{I}^{r_n \times r_n} - \mathbf{Q}_n)^{-1} \\ \mathbf{R}_1(\mathbf{I}^{r_1 \times r_1} - \mathbf{Q}_1)^{-1} & \mathbf{0}^{r_2 \times r_2} & \dots & \mathbf{0}^{r_n \times r_n} \\ \mathbf{R}'_2(\mathbf{I}^{r_2 \times r_2} - \mathbf{Q}_2)^{-1} & \dots & \dots & \dots \\ \dots & \dots & \dots & \dots \end{pmatrix}. \quad (\text{S13})$$

We mentioned in the main text that the positions of non-zero bars in the histograms are bounded by the smallest and largest values of $\Omega_{\alpha_{k+2}\alpha_{k+1}}$. More precisely, the positions of non-zero bars in the histograms for $\mathbb{P}(i|jS_k)$ are bounded by the smallest and largest elements in the block matrix

$$\begin{pmatrix} \mathbf{R}_j(\mathbf{I}^{r_j \times r_j} - \mathbf{Q}_j)^{-1} \\ \mathbf{R}'_j(\mathbf{I}^{r_j \times r_j} - \mathbf{Q}_j)^{-1} \end{pmatrix}, \quad (\text{S14})$$

which consists of the outward transition probabilities from microscopic states in j .

In the example shown in the main text, we have the effective transition matrix

$$\Omega = \begin{pmatrix} 0 & 4/7 & 3/7 & 1/7 & 0 & 0 & 0 \\ 1/2 & 0 & 0 & 0 & 4/9 & 1/6 & 1/18 \\ 1/2 & 0 & 0 & 0 & 1/3 & 1/2 & 1/6 \\ 0 & 0 & 0 & 0 & 2/9 & 1/3 & 7/9 \\ 0 & 11/49 & 3/49 & 1/49 & 0 & 0 & 0 \\ 0 & 6/49 & 15/49 & 5/49 & 0 & 0 & 0 \\ 0 & 4/49 & 10/49 & 36/49 & 0 & 0 & 0 \end{pmatrix}. \quad (\text{S15})$$

For the proof of convergence in Section (S3), we will assume the existence of an observable Markov state. For notational convenience, we enumerate microscopic states such that the observable Markov state is 1. Then we will define a transition matrix Ψ with the observable Markov state set as an absorbing state, and the other elements the same as in Ω

$$\Psi \equiv \mathbf{e}_1 \mathbf{e}_1^\top + \sum_{s=2}^n \mathbf{U}_s^\top \mathbf{R}_s (\mathbf{I} - \mathbf{Q}_s)^{-1} \mathbf{V}_s, \quad (\text{S16})$$

where we define $\mathbf{e}_1 = (1 \ 0 \ \dots \ 0)^\top$. We can write Ψ more explicitly in block form as

$$\Psi = \begin{pmatrix} 1 & \mathbf{R}_2(\mathbf{I}^{r_2 \times r_2} - \mathbf{Q}_2)^{-1} & \mathbf{R}_3(\mathbf{I}^{r_3 \times r_3} - \mathbf{Q}_3)^{-1} & \dots & \mathbf{R}_n(\mathbf{I}^{r_n \times r_n} - \mathbf{Q}_n)^{-1} \\ \mathbf{0}^{(m-1) \times 1} & \mathbf{0}^{r_2 \times r_2} & \mathbf{0}^{r_3 \times r_3} & \dots & \mathbf{0}^{r_n \times r_n} \\ \mathbf{R}'_2(\mathbf{I}^{r_2 \times r_2} - \mathbf{Q}_2)^{-1} & \dots & \mathbf{R}'_3(\mathbf{I}^{r_3 \times r_3} - \mathbf{Q}_3)^{-1} & \dots & \dots \\ \dots & \dots & \dots & \dots & \dots \end{pmatrix}. \quad (\text{S17})$$

Appendix S2: Detection of observable Markov state

In this section, we explore the possibility to detect practically an observable Markov state, which is a type of a “Markovian event” [1–3]. We will show that for an n -th order Markov process, we only need to check the Markov property up to n steps in the future and n steps in the past.

In the following calculation, we write $\{s_t\}_{t_1 \leq t \leq t_2}$ as $\{s\}_{t_2, t_1}$ for short. Note that the time points t_2, t_1 are written in a reverse order. We first recap the definition of a Markov state: for any $k > g \geq 1$, for any future sequence $\{s\}_{k, g+1}$ and history sequence $\{s\}_{g-1, 1}$, the observable Markov state γ satisfies

$$\mathbb{P}(\{s\}_{g, k+2} | s_{k+1} = \gamma; \{s\}_{k, 1}) = \mathbb{P}(\{s_t\}_{g, k+2} | s_{k+1} = \gamma). \quad (\text{S1})$$

For $g = k + 2$ (one step in the future) we can test with the method of histograms shown in the main text. We further discuss longer future sequences where $g \geq k + 3$. From the definition of conditional probability, we have the identity

$$\mathbb{P}(s_g | \{s\}_{g-1, k+2}; s_{k+1} = \gamma; \{s\}_{k, 1}) = \frac{\mathbb{P}(\{s\}_{g, k+2}; s_{k+1} = \gamma; \{s\}_{k, 1})}{\mathbb{P}(\{s\}_{g-1, k+1}; s_{k+1} = \gamma; \{s\}_{k, 1})} = \frac{\mathbb{P}(\{s\}_{g, k+2} | s_{k+1} = \gamma; \{s\}_{k, 1})}{\mathbb{P}(\{s\}_{g-1, k+2} | s_{k+1} = \gamma; \{s\}_{k, 1})}. \quad (\text{S2})$$

Now we *assume* that the observed dynamics is an n -th (definite) order Markov process. When the length of the sequence in the future satisfies $g - k - 1 \geq n$, i.e. $g - n \geq k + 1$, then for any s_g we can truncate the sequence in the condition from $\{s\}_{g-1,1}$ to $\{s\}_{g-1,g-n}$, and extend it to $\{s\}_{g-1,k+1}$ as

$$\mathbb{P}(s_g | \{s\}_{g-1,k+2}; s_{k+1} = \gamma; \{s\}_{k,1}) = \mathbb{P}(s_g | \{s\}_{g-1,g-n}) = \mathbb{P}(s_g | \{s\}_{g-1,k+2}; s_{k+1} = \gamma). \quad (\text{S3})$$

Given the condition in Eq. (S3), combining the identity in Eq. (S2), we have the statement

$$\mathbb{P}(\{s\}_{g-1,k+2} | s_{k+1} = \gamma; \{s\}_{k,1}) = \mathbb{P}(\{s\}_{g-1,k+2} | s_{k+1} = \gamma) \Rightarrow \mathbb{P}(\{s\}_{g,k+2} | s_{k+1} = \gamma; \{s\}_{k,1}) = \mathbb{P}(\{s\}_{g,k+2} | s_{k+1} = \gamma). \quad (\text{S4})$$

Note that the right-hand side of Eq. (S4) is the condition to test an observable Markov state. Thus, for an n -th order Markov process, we only need to check the condition in Eq. (S1) for $k \leq n$.

Appendix S3: Convergence of histograms

In this section, we prove that the histograms of transition probabilities conditioned on histories converge to a stationary distribution when the length of histories tends to infinity.

As introduced in the main text, we assume that there is at least one observable Markov state γ in the network. We split all possible history sequences S_k of length k into two disjoint sets depending on whether they have visited the observable Markov state γ or not, i.e. $\{S_k^j\} = \{S_k^j\}^M \cup \{S_k^j\}^N$, where

$$\begin{aligned} \{S_k^j\}^M &\equiv \{S_k^j | \exists t, 1 \leq t \leq k : s_t = \gamma\}; \\ \{S_k^j\}^N &\equiv \{S_k^j | \forall t, 1 \leq t \leq k : s_t \neq \gamma\}. \end{aligned} \quad (\text{S1})$$

The histogram is also decomposed into two parts $h_k(p) = h_k^M(p) + h_k^N(p)$. We will investigate the two parts separately in the following subsections.

1. Contribution from trajectories that visited the Markov state

In this subsection, we determine the contribution of $S_k^j \in \{S_k^j\}^M$ to the histogram $h(p)$ from $\mathbb{P}(i|jS_k^j) \in [p - \delta, p + \delta)$. The height of the bar contributed from $\{S_k^j\}^M$ at p is given by

$$h_k^M(p) = \frac{1}{\mathbb{P}(j)} \sum_{S_k^j \in \{S_k^j\}^M} \mathbb{P}(jS_k^j) \mathbb{1}_{[p-\delta, p+\delta)}[\mathbb{P}(i|jS_k^j)]. \quad (\text{S2})$$

For any $S_k^j \in \{S_k^j\}^M$, there exists the latest time step t_m where $s_{t_m} = \alpha_{t_m} = \gamma$, $s_{t > t_m} \neq \gamma$. Due to the definition of an observable Markov state, we can decompose the observable sequence probability $\mathbb{P}(\alpha_{k+1}S_k^j)$ into

$$\mathbb{P}(\alpha_{k+1}S_k^j) = \mathbb{P}(\alpha_{k+1}\{s_t\}_{t_m+1 \leq t \leq k} | s_{t_m} = \gamma) \mathbb{P}(\{s_t\}_{1 \leq t \leq t_m}). \quad (\text{S3})$$

We can substitute Eq. (S3) into the definition of the conditional probability in Eq. (2) of the main text to find

$$\begin{aligned} \mathbb{P}(i|jS_k^j) &= \frac{\sum_{\alpha_{k+1}} \mathbb{1}_j[\alpha_{k+1}] \mathbb{P}(\alpha_{k+1}S_k^j) \mathbb{P}(i|\alpha_{k+1})}{\sum_{\alpha_{k+1}} \mathbb{1}_j[\alpha_{k+1}] \mathbb{P}(\alpha_{k+1}S_k^j)} \\ &= \frac{\sum_{\alpha_{k+1}} \mathbb{1}_j[\alpha_{k+1}] \mathbb{P}(\alpha_{k+1}\{s_t\}_{t_m+1 \leq t \leq k} | s_{t_m} = \gamma) \mathbb{P}(i|\alpha_{k+1})}{\sum_{\alpha_{k+1}} \mathbb{1}_j[\alpha_{k+1}] \mathbb{P}(\alpha_{k+1}\{s_t\}_{t_m+1 \leq t \leq k} | s_{t_m} = \gamma)} \\ &= \mathbb{P}(i|j\{s_t\}_{t_m+1 \leq t \leq k} | \gamma), \end{aligned} \quad (\text{S4})$$

where $\mathbb{P}(i|\alpha_{k+1}) = \sum_{\alpha_{k+2}} \mathbb{1}_i[\alpha_{k+2}] \mathbb{P}(\alpha_{k+2}|\alpha_{k+1})$. Eq. (S4) is an important step in our calculation: the probability of early histories $\mathbb{P}(\{s_t\}_{1 \leq t \leq t_m})$ is cancelled because it does not depend on k or α_{k+1} , i.e. it is the same in every term in the summation. Therefore, the $\mathbb{P}(i|jS_k^j)$ is determined only by the steps after t_m in the history, i.e. by $\{s_t\}_{t_m \leq t \leq k+2}$. Intuitively, this is because the memory resets after visiting the observable Markov state.

We can extend the history l steps further to the past to be $S_{k+l}^j \equiv \{s_t\}_{-l+1 \leq t \leq k}$, $l \geq 1$, and define $\{S_{k+l}^j\}^M$ as the trajectories that do *not* visit γ in the last k steps during $\{s_t\}_{1 \leq t \leq k}$. The contributions to the histogram from

$\{S_k^j\}^M$ and $\{S_{k+l}^j\}^M$ are exactly the same, for they have the same possible sequences $\{s_t\}_{1 \leq t \leq k+2}$. Thus, for any $S_{k+l}^j = \{s_t\}_{-l+1 \leq t \leq k} \in \{S_{k+l}^j\}^M$, we have $\mathbb{P}(i|j\{s_t\}_{-l+1 \leq t \leq k}) = \mathbb{P}(i|j\{s_t\}_{1 \leq t \leq k})$. Since $\mathbb{P}(i|jS_k^j)$ is only affected by the last $(k - t_m)$ steps of the history, $h_k^M(p)$ also does not depend on the earlier history. We can determine the height of bars for $\{S_{k+l}^j\}^M$ as

$$\begin{aligned} h_{k+l}^M(p) &= \frac{1}{\mathbb{P}(j)} \sum_{\{s_t\}_{1 \leq t \leq k} \in \{S_k^j\}^M} \sum_{\{s_t\}_{-l+1 \leq t \leq 0}} \mathbb{P}(jS_{k+l}^j) \mathbb{1}_{[p-\delta, p+\delta)} [\mathbb{P}(i|jS_{k+l}^j)] \\ &= \frac{1}{\mathbb{P}(j)} \sum_{\{s_t\}_{1 \leq t \leq k} \in \{S_k^j\}^M} \mathbb{P}(jS_k^j) \mathbb{1}_{[p-\delta, p+\delta)} [\mathbb{P}(i|jS_k^j)] = h_k^M(p). \end{aligned} \quad (\text{S5})$$

We have proved that the contribution from sequences $S_k^j \in \{S_k^j\}^M$ is already stationary, i.e. does not change in the histograms for longer histories.

2. Contribution from trajectories that did not visit the Markov state

In this subsection, we prove that the total contribution from $S_k^j \in \{S_k^j\}^N$ to the histogram with L bars

$$\sum_{z=0}^L h_k^N(p = 2z\delta) = \frac{1}{\mathbb{P}(j)} \sum_{S_k^j \in \{S_k^j\}^N} \mathbb{P}(jS_k^j) \quad (\text{S6})$$

vanishes as k tends to infinity, where we expressed the positions of bars as $p = 2z\delta$, $0 \leq z \leq L$, $2L\delta = 1$.

Trajectories with $\alpha_{k+1} = \gamma$ are trivial because the history S_k^j does not matter. Thus, in the following calculation, we choose j *not* being an observable Markov state, i.e. $\alpha_{k+1} \neq \gamma$. For notational convenience (and w.l.o.g.), we enumerate microscopic states such that the observable Markov state $\gamma = 1$. We introduce the transition matrix Ψ with absorbing boundary condition at 1 as in Eq. (S16, S17).

We define column vectors $\mathbf{e}_i \equiv (0 \dots 0 \mathbf{1} 0 \dots 0)^\top$ with the i -th element being 1, and the steady state distribution of Ω as $\boldsymbol{\pi}$, which satisfies $\Omega \boldsymbol{\pi} = \boldsymbol{\pi}$. The probability of starting from a steady state distribution $\boldsymbol{\pi}$, ending in α_{k+1} , and not visiting γ between step 1 and $k+1$ is given by

$$\mathbb{P}(\alpha_{k+1}; \forall t \in [1, k+1], \alpha_t \neq \gamma) = \mathbf{e}_{\alpha_{k+1}}^\top \Psi^{k+1} \boldsymbol{\pi}. \quad (\text{S7})$$

Therefore, we have

$$\frac{1}{\mathbb{P}(j)} \sum_{S_k^j \in \{S_k^j\}^N} \mathbb{P}(jS_k^j) = \frac{1}{\pi(j)} \sum_{\alpha_{k+1}} \mathbb{1}_j[\alpha_{k+1}] \mathbb{P}(\alpha_{k+1}; \forall t, \alpha_t \neq \gamma) = \frac{1}{\pi(j)} \sum_{\alpha_{k+1}} \mathbb{1}_j[\alpha_{k+1}] \mathbf{e}_{\alpha_{k+1}}^\top \Psi^{k+1} \boldsymbol{\pi}. \quad (\text{S8})$$

Since $\Psi^{k+1} \boldsymbol{\pi}$ has non-negative components and because $\alpha_{k+1} \neq 1$, we can replace the projection to a sum over all the states except γ to obtain an inequality

$$\sum_{\alpha_{k+1}} \mathbb{1}_j[\alpha_{k+1}] \mathbf{e}_{\alpha_{k+1}}^\top \Psi^{k+1} \boldsymbol{\pi} \leq (\mathbf{0} \ \mathbf{1}^\top) \Psi^{k+1} \boldsymbol{\pi}, \quad (\text{S9})$$

where $\mathbf{1}$ denotes an $(m-1) \times 1$ all-one column vector. The right hand side of Eq. (S9) indicates a process starting from the stationary distribution of Ω , changing state 1 to an absorbing state, and letting the system evolve for $k+1$ steps. What we are actually evaluating is the sum of probabilities that the system does not end in 1, i.e. the survival probability in the rest of the network.

A finite Markov chain has its eigenvalue with the second largest modulus satisfying $|\lambda_1| < 1$ if and only if it is indecomposable and aperiodic [4, 5] (note that the statement is more general than the Perron–Frobenius theorem. The later does not apply to indecomposable but reducible matrices, e.g. Markov chains with only one absorbing state). The Markov chain Ψ with one absorbing state is indecomposable and aperiodic if the original Markov chain Ω is irreducible. Therefore, we can write the generalized eigenvalues of Ψ as $\lambda_0 = 1 > |\lambda_1| \geq |\lambda_2| \geq \dots \geq |\lambda_{m-1}|$. We have the Jordan decomposition of the matrix $\Psi = \mathbf{S} \mathbf{D} \mathbf{S}^{-1}$. Columns of \mathbf{S} are generalized right eigenvectors \mathbf{u} and rows of \mathbf{S}^{-1} are generalized left eigenvectors \mathbf{v} of Ψ .

We denote the stationary distribution of the absorbing Markov chain with transition matrix Ψ as $\boldsymbol{\mu}_0 = (1 \ 0 \ \dots \ 0)^\top$, and the probability distribution after evolving for $t \geq 1$ steps as $\boldsymbol{\mu}_t = \Psi^t \boldsymbol{\pi}$. From the convergence theorem of a Markov chain [6], we have

$$\max_r |\mu_{k+1}(r) - \pi(r)| \leq M |\lambda_1|^{k+1-m^*} \binom{k+1}{m^*-1}, \quad (\text{S10})$$

where m^* is the dimension of the largest Jordan block among all generalized eigenvalues. The constant M is given by

$$M = \max_i \sum_{L=1}^{R-1} \sum_{q=0}^{n_L-1} \sum_{l=S_L+1}^{S_L+n_L-q} \sum_{j=1}^m |u_{l-1}(i) v_{l+q-1}(j)|, \quad (\text{S11})$$

where R is the total number of Jordan blocks, n_L is the size of the Jordan block \mathbf{J}_L , $S_L = \sum_{s=0}^{L-1} n_s$, $1 \leq L \leq R-1$, $S_0 = 1$, and \mathbf{u} and \mathbf{v} are generalized right and left eigenvectors of Ψ . Therefore, the total variation distance between $\boldsymbol{\mu}_{k+1}$ and $\boldsymbol{\mu}_0$ is bounded by

$$\|\boldsymbol{\mu}_{k+1} - \boldsymbol{\mu}_0\|_{\text{TV}} = \frac{1}{2} \sum_{r=1}^m |\mu_{k+1}(r) - \mu_0(r)| \leq C' |\lambda_1|^{k+1-m^*} \binom{k+1}{m^*-1}, \quad (\text{S12})$$

where we choose $C' = Mm/2$. On the other hand, we have

$$\sum_{r=1}^m |\mu_{k+1}(r) - \mu_0(r)| = 1 - \mu_{k+1}(m) + \sum_{r=2}^m \mu_{k+1}(r) = 1 - \mu_{k+1}(m) + (0 \ \mathbf{1}^\top) \Psi^{k+1} \boldsymbol{\pi} \geq (0 \ \mathbf{1}^\top) \Psi^{k+1} \boldsymbol{\pi}. \quad (\text{S13})$$

Combining Eqs. (S9,S12,S13) we have the bound

$$\sum_{z=0}^L h_k^{\text{N}}(p = 2z\delta) \leq \frac{1}{\pi(j)} (0 \ \mathbf{1}^\top) \Psi^{k+1} \boldsymbol{\pi} \leq \frac{1}{\pi(j)} \sum_{r=1}^m |\mu_{k+1}(r) - \mu_0(r)| \leq C |\lambda_1|^{k+1-m^*} \binom{k+1}{m^*-1}, \quad (\text{S14})$$

where $C = 2C'/\pi(j)$.

The bound in Eq. (S14) vanishes as $k \rightarrow \infty$ because $|\lambda_1|^k$ decays faster than the combinatorial grows with k . We can show the limit explicitly by taking the logarithm

$$\ln \left[|\lambda_1|^{k+1-m^*} \binom{k+1}{m^*-1} \right] = (k+1-m^*) \ln(|\lambda_1|) + \ln \left[\frac{(k+1)!}{(m^*-1)!(k-m^*+2)} \right]. \quad (\text{S15})$$

Then we insert the bounds [7] for factorials $\sqrt{2\pi n} n^{n+\frac{1}{2}} e^{-n} < n! \leq n^{n+\frac{1}{2}} e^{-n+1}$ to bound these as

$$\ln \left[\frac{(k+1)!}{(k-m^*+2)!} \right] < \left(k + \frac{3}{2} \right) \ln(k+1) - k - \ln(2\pi) + k - m^* + 2 - \left(k - m^* + \frac{5}{2} \right) \ln(k - m^* + 2) \leq (m^* - 1) \ln(k+1) - m^* + 2 - \ln(2\pi), \quad (\text{S16})$$

where we have inserted $m^* \geq 1$. Comparing the first term in Eq. (S15) and Eq. (S16), the two terms depending on k are $(k+1-m^*) \ln(|\lambda_1|)$ and $(m^*-1) \ln(k+1)$, and the other terms are constants. The sum of the two relevant terms goes to negative infinity when k goes to infinity, because a linear function of x grows faster than a logarithm. Therefore, the bound in Eq. (S14) goes to zero when k goes to infinity.

Specifically, if the matrix Ψ is diagonalizable, we have the bound

$$\sum_{z=0}^L h_k^{\text{N}}(p = 2z\delta) = \frac{1}{\mathbb{P}(j)} \sum_{S_k^j \in \{S_k^j\}^{\text{N}}} \mathbb{P}(j S_k^j) \leq C |\lambda_1|^k. \quad (\text{S17})$$

Therefore, if Ψ is diagonalizable, the total contribution from $\{S_k^j\}^{\text{N}}$ decays as a power of $|\lambda_1| < 1$ when k becomes large.

For a fixed k , the contribution from $\{S_{k+l}^j\}^{\text{M}}$ is independent of l as calculated in subsection S3.1, and that from $\{S_{k+l}^j\}^{\text{N}}$ still changes with l . Denote the ‘‘stationary’’ histogram as \mathbf{h}_∞ , then the total variation distance (TVD)

between \mathbf{h}_k and \mathbf{h}_∞ is bounded by the contribution from $\{S_{k+l}^j\}^N$

$$\begin{aligned}
\|\mathbf{h}_k - \mathbf{h}_\infty\|_{\text{TV}} &= \frac{1}{2} \sum_{z=0}^L |h_k(z) - h_\infty(z)| \\
&= \frac{1}{2} \sum_{z=0}^L |h_k(z) - h_k^{\text{M}}(z) - h_\infty(z) + h_\infty^{\text{M}}(z)| \\
&= \frac{1}{2} \sum_{z=0}^L |h_k^{\text{N}}(z) - h_\infty^{\text{N}}(z)| \leq \sum_{z=0}^L h_k^{\text{N}}(z) \leq C|\lambda_1|^{k+1-m^*} \binom{k+1}{m^*-1},
\end{aligned} \tag{S18}$$

where we have written $h(p = 2z\delta)$ as $h(z)$ for short and used $h_k^{\text{M}}(z) = h_\infty^{\text{M}}(z)$ in the second step.

In conclusion, we proved that the contribution from $\{S_k^j\}^{\text{M}}$ is stationary, and that $\{S_k^j\}^{\text{N}}$ vanishes as k tends to infinity. This proves that the histograms converge to a stationary distribution.

-
- [1] J. van der Meer, J. Degünther, and U. Seifert, *Phys. Rev. Lett.* **130**, 257101 (2023).
 - [2] J. Degünther, J. van der Meer, and U. Seifert, *Phys. Rev. Res.* **6**, 023175 (2024).
 - [3] J. Degünther, J. van der Meer, and U. Seifert, *Proc. Natl. Acad. Sci.* **121**, e2405371121 (2024).
 - [4] K. R. Garren, *Bounds for the Eigenvalues of a Matrix*, Vol. 4373 (National Aeronautics and Space Administration, 1968).
 - [5] J. S. Rosenthal, *SIAM Rev.* **37**, 387 (1995).
 - [6] T. M. Silva, L. Silva, and S. Fernandes, *Linear Algebra Appl.* **488**, 199 (2016).
 - [7] H. Robbins, *Amer. Math. Monthly* **62**, 26 (1955).